Near-Surface Full Waveform Inversion Reveals Bedrock Controls on Critical Zone Architecture

B.J. Eppinger[1], W.S. Holbrook[1], Z. Liu[2], B.A. Flinchum[3], J. Tromp[4,5]

[1]Department of Geosciences, Virginia Polytechnic Institute and State University, Blacksburg, VA, USA

[2]Ocean University of China, Qingdao, China; Previously, Department of Geosciences, Princeton University, Princeton, NJ, USA

[3]Clemson University, Environmental Engineering and Earth Sciences, Clemson, SC, USA

[4]Department of Geosciences, Princeton University, Princeton, NJ, USA

[5]Program in Applied & Computational Mathematics, Princeton University, Princeton, NJ 08544-1000, USA

Contents of this file

Figures S1 to S7

Introduction

Here we present supplementary data pertaining to our source time function estimation and full waveform inversion results. Specifically, Figure S1 shows all 20 of the estimated source time functions. Figures S2 to S4 show waveform fits before and after each stage of the multiscale surface wave inversion. Similarly, Figures S5 to S7 show waveforms fits before and after each stage of the multiscale body wave inversion.
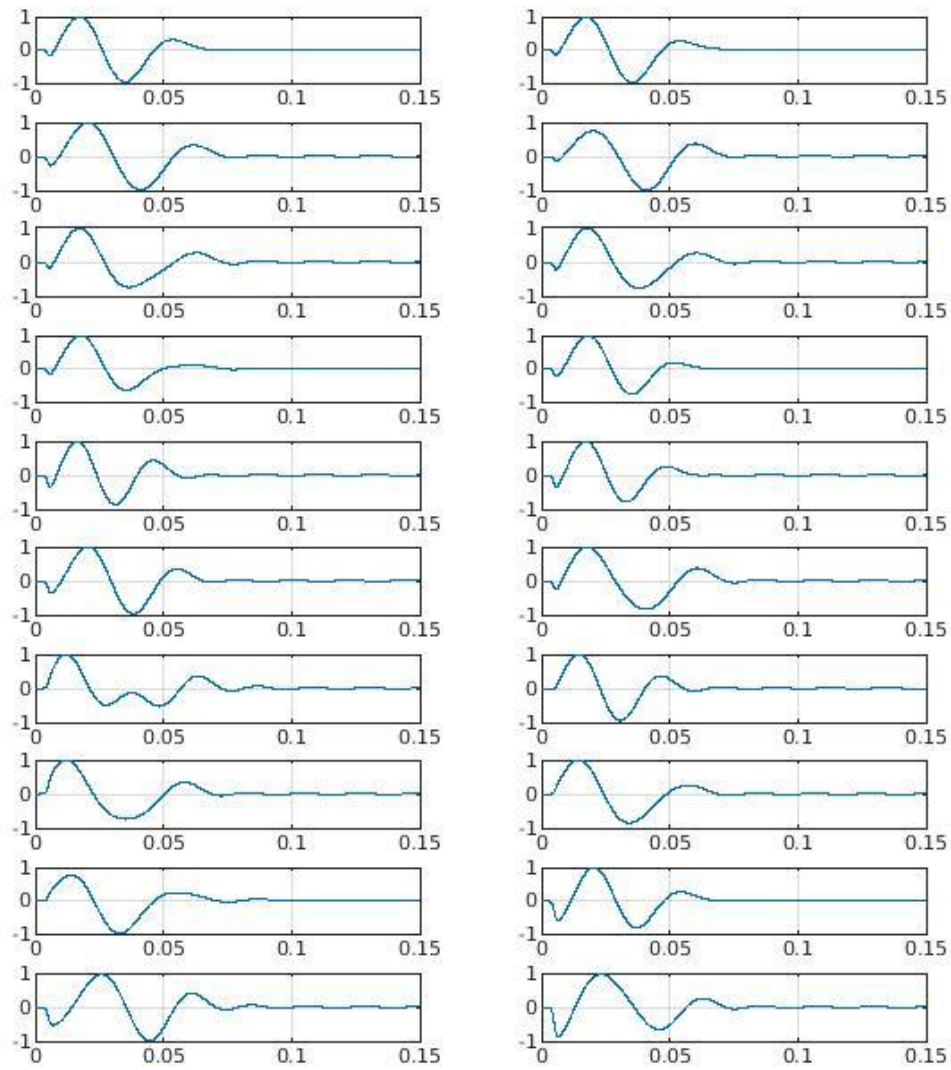
Figure S1. All 20 of the source time functions estimated using the method described in section 3.2 of the main text. Note the general similarity of each source time function to others implying consistent quality in the data and estimation process.
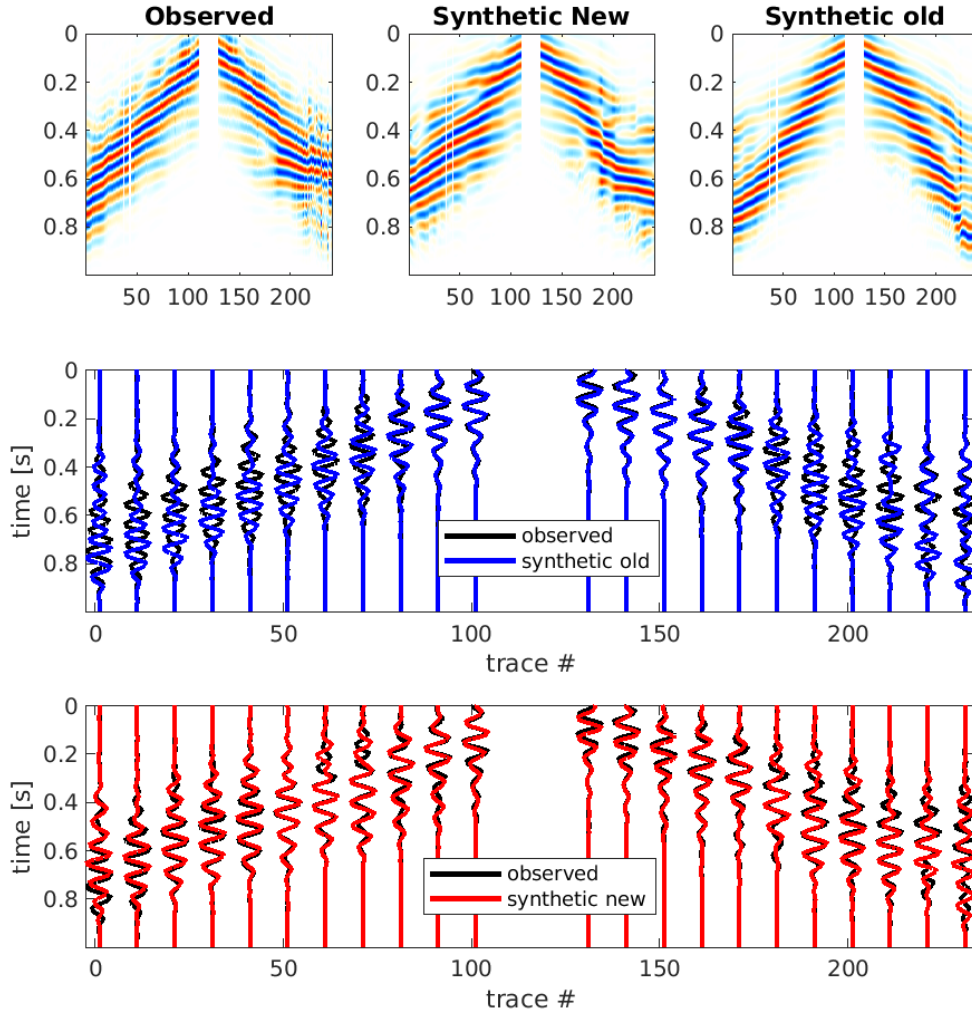
Figure S2. Waveform comparisons of preprocessed data for the 6-14 Hz stage of the surface wave multiscale strategy. The top three panels show shot gathers of observed data, synthetic waveforms after applying FWI for 15 iterations, and the synthetic waveforms corresponding to the model derived with surface wave dispersion inversion. The middle panel shows waveform comparison of every 10th trace for observed data and synthetic data corresponding to the model derived with surface wave dispersion inversion. The bottom panel shows waveform comparison of every 10th trace for observed data and synthetic data corresponding to the model derived after 15 iterations of FWI.
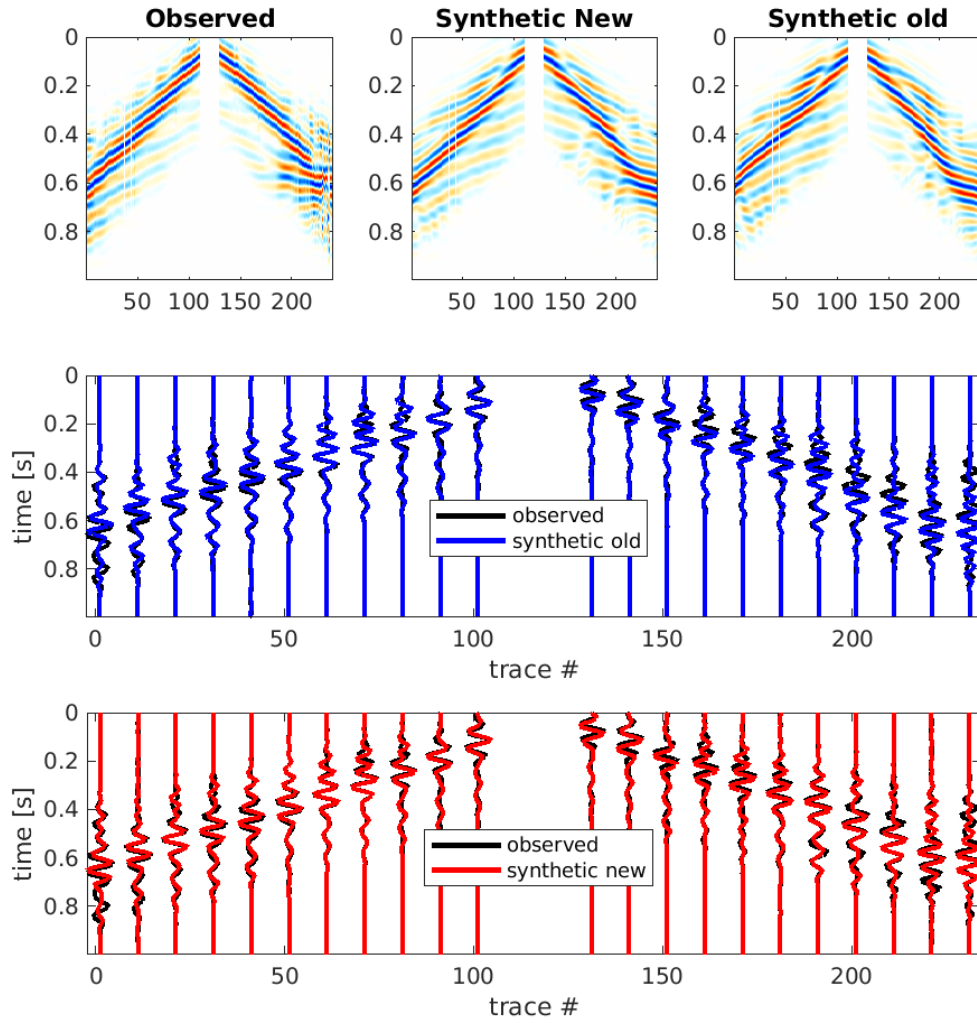
Figure S3. Waveform comparisons of preprocessed data for the 6-18 Hz stage of the surface wave multiscale strategy. The top three panels show shot gathers of observed data, synthetic waveforms after applying FWI for 30 iterations, and the synthetic waveforms corresponding to the model derived after applying FWI for 15 iterations. The middle panel shows waveform comparison of every 10th trace for observed data and synthetic data corresponding to the model derived after applying FWI for 15 iterations. The bottom panel shows waveform comparison of every 10th trace for observed data and synthetic data corresponding to the model derived after 30 iterations of FWI.
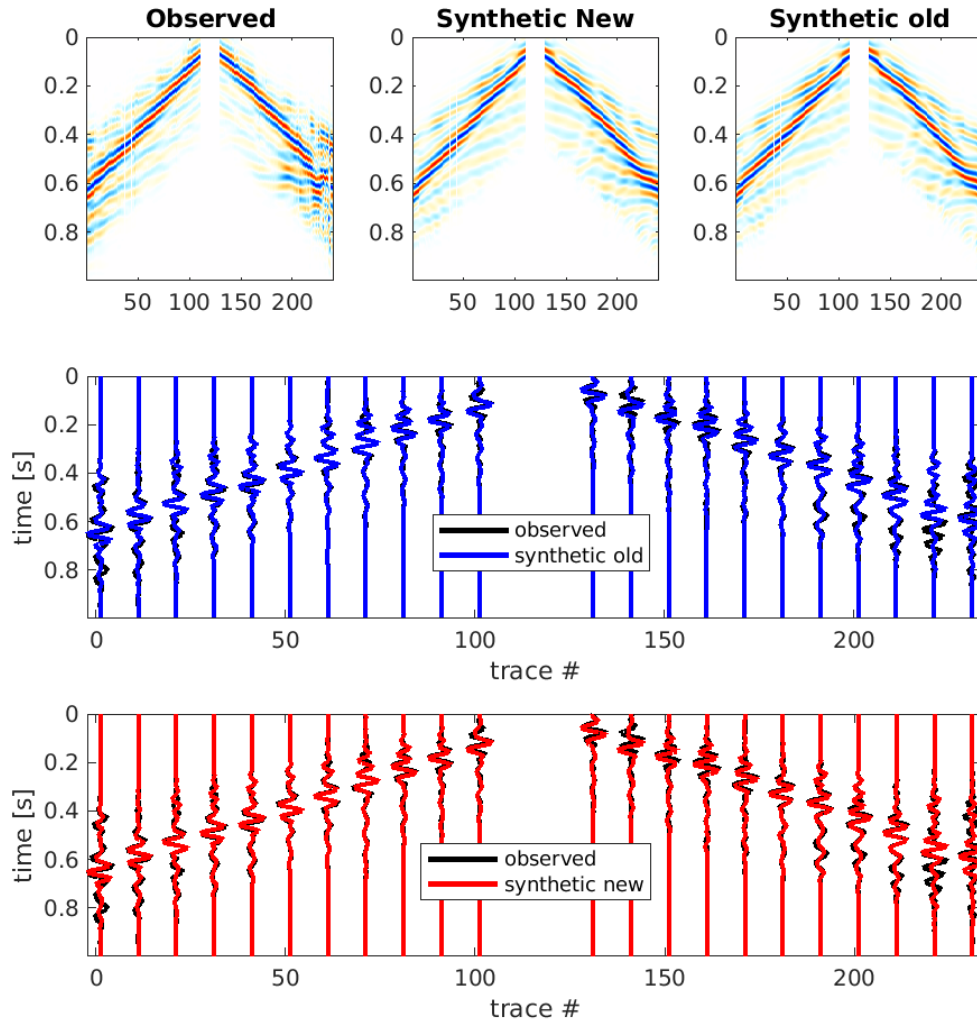
Figure S4. Waveform comparisons of preprocessed data for the 6-22 Hz stage of the surface wave multiscale strategy. The top three panels show shot gathers of observed data, synthetic waveforms after applying FWI for 45 iterations, and the synthetic waveforms corresponding to the model derived after applying FWI for 30 iterations. The middle panel shows waveform comparison of every 10th trace for observed data and synthetic data corresponding to the model derived after applying FWI for 30 iterations. The bottom panel shows waveform comparison of every 10th trace for observed data and synthetic data corresponding to the model derived after 45 iterations of FWI.
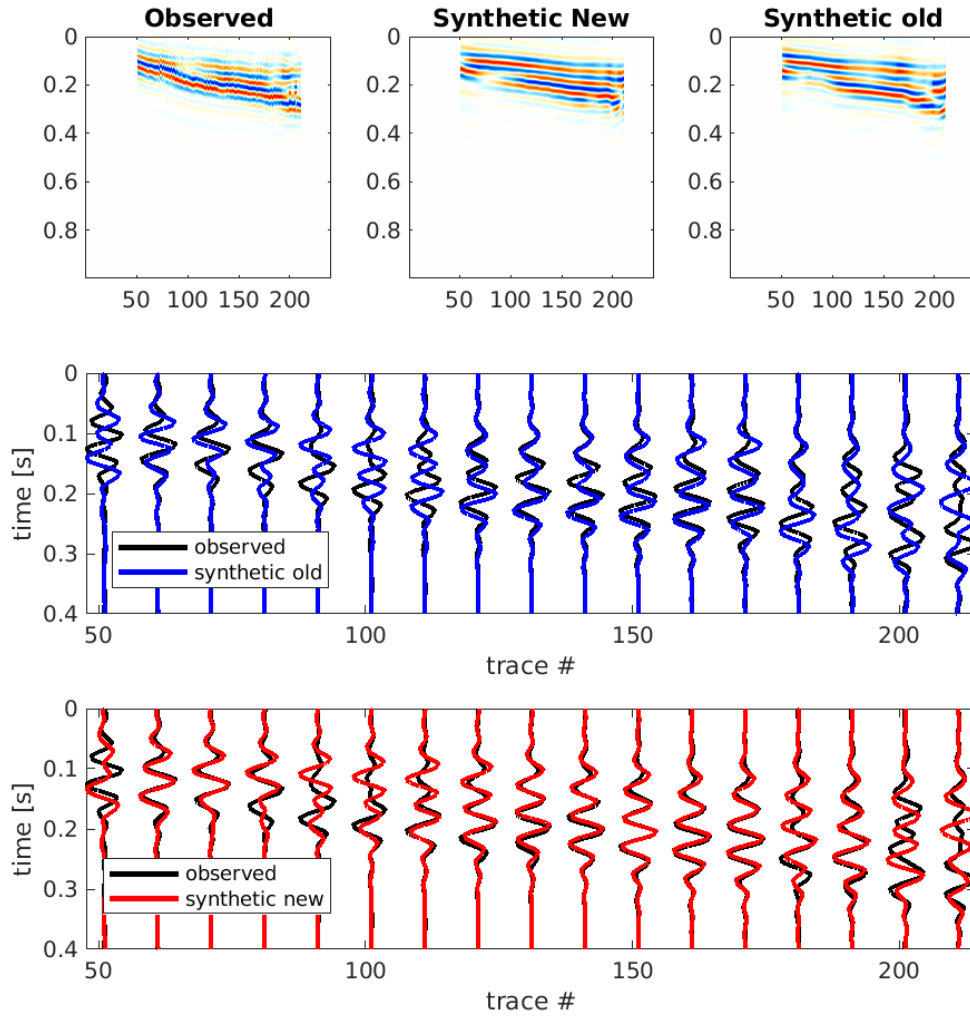
Figure S5. Waveform comparisons of preprocessed data for the 8-24 Hz stage of the body wave multiscale strategy. The top three panels show shot gathers of observed data, synthetic waveforms after applying FWI for 20 iterations, and the synthetic waveforms corresponding to the model derived with ray-based travel time tomography. The middle panel shows waveform comparison of every 10th trace for observed data and synthetic data corresponding to the model derived with ray-based travel time tomography. The bottom panel shows waveform comparison of every 10th trace for observed data and synthetic data corresponding to the model derived after 20 iterations of FWI.
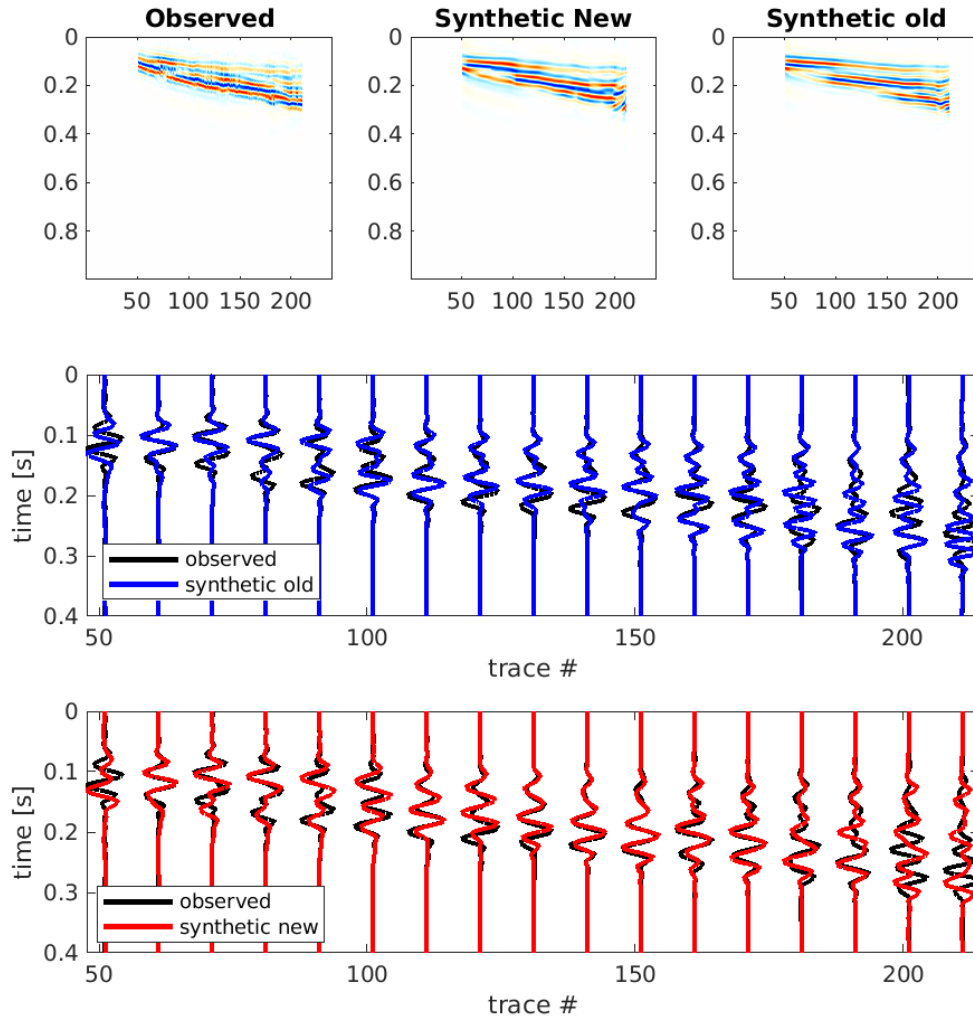
Figure S6. Waveform comparisons of preprocessed data for the 8-40 Hz stage of the body wave multiscale strategy. The top three panels show shot gathers of observed data, synthetic waveforms after applying FWI for 60 iterations, and the synthetic waveforms corresponding to the model derived after applying FWI for 20 iterations. The middle panel shows waveform comparison of every 10th trace for observed data and synthetic data corresponding to the model derived after applying FWI for 20 iterations. The bottom panel shows waveform comparison of every 10th trace for observed data and synthetic data corresponding to the model derived after 60 iterations of FWI.
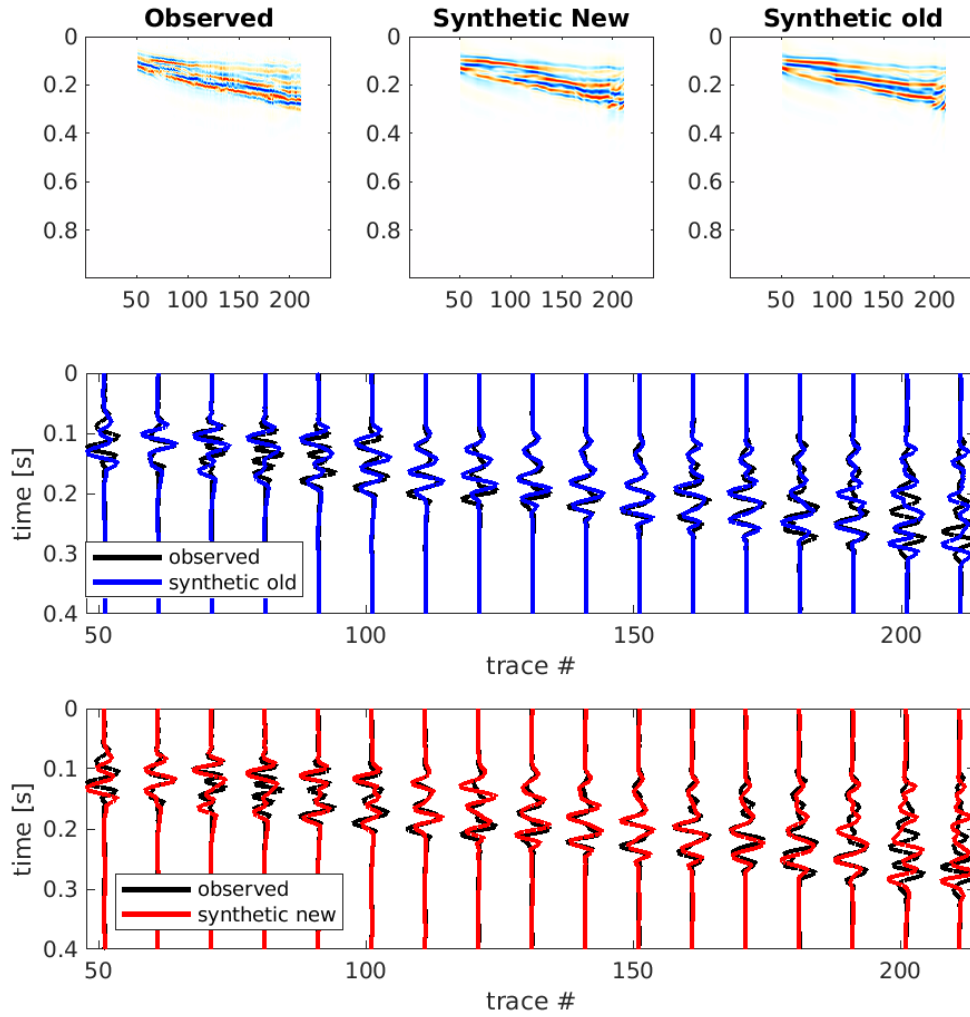
Figure S7. Waveform comparisons of preprocessed data for the 8-56 Hz stage of the body wave multiscale strategy. The top three panels show shot gathers of observed data, synthetic waveforms after applying FWI for 100 iterations, and the synthetic waveforms corresponding to the model derived after applying FWI for 60 iterations. The middle panel shows waveform comparison of every 10th trace for observed data and synthetic data corresponding to the model derived after applying FWI for 60 iterations. The bottom panel shows waveform comparison of every 10th trace for observed data and synthetic data corresponding to the model derived after 100 iterations of FWI.